

- Fortey *et al.*, *Geol. Surv. Can. Pap.* **90-9**, 5 (1991); and R. A. Fortey, D. A. T. Harper, J. K. Ingham, A. W. Owen, A. W. A. Rushton, *Geol. Mag.* **132**, 15 (1995).
11. R. E. Denison, W. H. Burke, J. B. Otto, E. A. Hetherington, in *Symposium on the Geology of the Ouachita Mountains, Volume I*, C. G. Stone, Ed. (Arkansas Geological Commission, Little Rock, AR, 1977), pp. 25–40.
 12. J. Rodgers, in *Studies of Appalachian Geology: Northern and Maritime*, E. Zen, W. S. White, J. B. Hadley, J. B. Thompson Jr., Eds. (Interscience, New York, 1968), pp. 141–149; J. Reinhardt, *Mod. Geol. Surv. Rep. Invest.* **23** (1974); R. W. Pfeil and J. F. Read, *J. Sediment. Petrol.* **50**, 91 (1980).
 13. G. W. Viele and W. A. Thomas, in *The Appalachian-Ouachita Orogen in the United States*, R. D. Hatcher Jr., W. A. Thomas, G. W. Viele, Eds., vol. F-2 of *The Geology of North America* (Geological Society of America, Boulder, CO, 1989), pp. 695–728.
 14. G. R. Keller *et al.*, *Geology* **17**, 119 (1989).
 15. S. A. Bowring and W. J. Hoppe, *Okla. Geol. Surv. Guideb.* **21**, 54 (1982); D. D. Lambert, D. M. Unruh, M. C. Gilbert, *Geology* **16**, 13 (1988); J. P. Hogan *et al.*, *Geol. Soc. Am. Abstr. Progr.* **28** (no. 1), 19 (1996).
 16. D. A. McConnell and M. C. Gilbert, *Okla. Geol. Surv. Guideb.* **23**, 11 (1986).
 17. W. E. Ham *et al.*, *Okla. Geol. Surv. Bull.* **95** (1964).
 18. W. A. Thomas, in *Sedimentary Cover—North American Craton: U.S.*, L. L. Sloss, Ed., vol. D-2 of *The Geology of North America* (Geological Society of America, Boulder, CO, 1988), pp. 471–492.
 19. D. E. Raymond, *Ala. Geol. Surv. Bull.* **143** (1991).
 20. F. F. Mellen, *Am. Assoc. Pet. Geol. Bull.* **61**, 1897 (1977).
 21. C. E. Resser, *Geol. Soc. Am. Spec. Pap.* **15** (1938); J. G. Grohskopf, *Mo. Geol. Surv.* **37** (1955); A. R. Palmer, *U.S. Geol. Surv. Prof. Pap.* **374-F** (1962).
 22. K. S. Johnson *et al.*, in *Sedimentary Cover—North American Craton: U.S.*, L. L. Sloss, Ed., vol. D-2 of *The Geology of North America* (Geological Society of America, Boulder, CO, 1988), pp. 307–359.
 23. J. L. Wilson, *J. Paleontol.* **28**, 249 (1954); V. E. Barnes, *Univ. Tex. Bur. Econ. Geol. Pub.* **592A**, 11 (1959); R. L. Ethington, S. C. Finney, J. E. Repetski, in *The Appalachian-Ouachita Orogen in the United States*, R. D. Hatcher Jr., W. A. Thomas, G. W. Viele, Eds., vol. F-2 of *The Geology of North America* (Geological Society of America, Boulder, CO, 1989), pp. 563–574.
 24. A. R. Palmer *et al.*, *Geology* **12**, 91 (1984).
 25. W. A. Thomas, *Am. Assoc. Pet. Geol. Bull.* **56**, 81 (1972).
 26. L. Alberstadt and J. E. Repetski, *Palaio* **4**, 225 (1989).
 27. J. Abbruzzi, S. M. Kay, M. E. Bickford, *12th Congreso Geológico Argentino y 2nd Congreso de Exploración de Hidrocarburos* **3**, 331 (1993); S. M. Kay, in *International Geological Correlation Program Project 376 (Laurentian-Gondwana Connections before Pangea)*, *International Meeting and Field Conference Abstracts with Programs*, V. A. Ramos, Ed. (1995), pp. 19–20.
 28. R. A. Astini, in *Ordovician Odyssey: 7th International Symposium on the Ordovician System*, J. D. Cooper, M. L. Droser, S. C. Finney, Eds. (Pacific Section, Society of Economic Paleontologists and Mineralogists, Book 77, Fullerton, CA, 1995), pp. 217–220.
 29. R. A. Astini *et al.*, *Geol. Soc. Am. Abstr. Progr.* **27** (no. 6), A-458 (1995).
 30. F. Cañas, in *Ordovician Odyssey: 7th International Symposium on the Ordovician System*, J. D. Cooper, M. L. Droser, S. C. Finney, Eds. (Pacific Section, Society of Economic Paleontologists and Mineralogists, Book 77, Fullerton, CA, 1995), pp. 221–224.
 31. L. R. Sternbach and G. M. Friedman, *Soc. Econ. Paleontol. Mineral. Core Workshop* **5**, 2 (1984).
 32. F. Cañas and M. Carrera, *Facies* **29**, 169 (1993); M. Keller, O. Bordonaro, F. Cañas, *12th Congreso Geológico Argentino y 2nd Congreso de Exploración de Hidrocarburos* **1**, 235 (1993).
 33. D. F. Toomey and W. E. Ham, *J. Paleontol.* **41**, 981 (1967); D. F. Toomey and M. H. Nitecki, *Fieldiana (New Ser.)* **2** (1979).
 34. R. A. Astini, in *Ordovician Odyssey: 7th International Symposium on the Ordovician System*, J. D. Cooper, M. L. Droser, S. C. Finney, Eds. (Pacific Section, Society of Economic Paleontologists and Mineralogists, Book 77, Fullerton, CA, 1995), pp. 177–180.
 35. J. L. Benedetto *et al.*, *ibid.*, pp. 181–184.
 36. N. E. Vaccari, *ibid.*, pp. 193–196.
 37. J. L. Benedetto, *12th Congreso Geológico Argentino y 2nd Congreso de Exploración de Hidrocarburos* **3**, 375 (1993); N. E. Vaccari, thesis, Universidad Nacional de Córdoba, Argentina (1994).
 38. R. A. Astini, V. Ramos, J. L. Benedetto, N. E. Vaccari, F. Cañas, *13th Congreso Geológico Argentino y 3rd Congreso de Exploración de Hidrocarburos*, in press.
 39. G. L. Albanesi, J. L. Benedetto, P. Y. Gagnier, *Bol. Acad. Nac. Cienc. Córdoba Argent.* **60**, 519 (1995).
 40. J. L. Benedetto and T. M. Sánchez, in *International Geological Correlation Program Project 351, 2nd International Meeting Abstracts, Early Paleozoic Evolution in Northwest Gondwana*, N. Hamoumi, Ed. (1994), pp. 143–144.
 41. J. W. Valentine, *System. Zool.* **20**, 253 (1971); *Evolutionary Paleogeology of Marine Biosfera* (Prentice-Hall, Englewood Cliffs, NJ, 1973); J. A. Talent, in *Ekostratigrafiya, Paleobiogeografiya i Stratigraficheskie Granitsy*, *14th Pacific Science Congress*, K. V. Simakov, Ed. (Akademii Nauk, Moscow, 1985), pp. 54–90; J. A. Talent, R. T. Gratsianov, E. A. Yolkina, *Int. Symp. Shallow Tethys* **2**, 87 (1986).
 42. R. A. Astini, thesis, Universidad Nacional de Córdoba, Argentina (1991); G. González Bonorino and F. González Bonorino, *Rev. Geol. Chile* **18**, 97 (1991); R. A. Astini, *Bol. R. Soc. Esp. Hist. Nat. Secc. Geol.* **88**, 113 (1993).
 43. W. D. Huff, S. M. Bergström, D. R. Kolata, C. Cingolani, D. W. Davis, in *Ordovician Odyssey: 7th International Symposium on the Ordovician System*, J. D. Cooper, M. L. Droser, S. C. Finney, Eds. (Pacific Section, Society of Economic Paleontologists and Mineralogists, Book 77, Fullerton, CA, 1995), pp. 343–349.
 44. R. T. Buffler and W. A. Thomas, in *Phanerozoic Evolution of North American Continent-Ocean Transitions, Continent-Ocean Transect Volume*, R. C. Speed, Ed. (Geological Society of America, Boulder, CO, 1994), pp. 219–264.
 45. We thank C. J. Schmidt for stimulating our collaboration in this research and for discussing these ideas with both of us, J. L. Benedetto and N. E. Vaccari for discussions of paleobiogeography of Precambrian faunas, N. Rast for comments on an early draft of this manuscript, and S. J. Juszczuk for preparation of the illustrations.

RESEARCH ARTICLE

Evidence for Widespread ^{26}Al in the Solar Nebula and Constraints for Nebula Time Scales

S. S. Russell, G. Srinivasan, G. R. Huss, G. J. Wasserburg, G. J. MacPherson*

A search was made for ^{26}Mg ($^{26}\text{Mg}^*$) from the decay of ^{26}Al (half-life = 0.73 million years) in Al-rich objects from unequilibrated ordinary chondrites. Two Ca-Al-rich inclusions (CAIs) and two Al-rich chondrules (not CAIs) were found that contained ^{26}Al when they formed. Internal isochrons for the CAIs yielded an initial $^{26}\text{Al}/^{27}\text{Al}$ ratio [$(^{26}\text{Al}/^{27}\text{Al})_0$] of 5×10^{-5} , indistinguishable from most CAIs in carbonaceous chondrites. This result shows that CAIs with this level of ^{26}Al are present throughout the classes of chondrites and strengthens the notion that ^{26}Al was widespread in the early solar system. The two Al-rich chondrules have lower $^{26}\text{Mg}^*$, corresponding to a $(^{26}\text{Al}/^{27}\text{Al})_0$ ratio of $\sim 9 \times 10^{-6}$. Five other Al-rich chondrules contain no resolvable $^{26}\text{Mg}^*$. If chondrules and CAIs formed from an isotopically homogeneous reservoir, then the chondrules with ^{26}Al must have formed or been last altered ~ 2 million years after CAIs formed; the $^{26}\text{Mg}^*$ -free chondrules formed >1 to 3 million years later still. Because $^{26}\text{Mg}^*$ -containing and $^{26}\text{Mg}^*$ -free chondrules are both found in Chainpur, which was not heated to more than $\sim 400^\circ\text{C}$, it follows that parent body metamorphism cannot explain the absence of $^{26}\text{Mg}^*$ in some of these chondrules. Rather, its absence indicates that the lifetime of the solar nebula over which CAIs and chondrules formed extended over ~ 5 million years.

The short-lived radionuclide ^{26}Al was present 4.56 gigayears ago in Ca-Al-rich inclusions (CAIs), which are preserved in primitive meteorites (1–4). The inferred initial abundance of ^{26}Al (giving a $^{26}\text{Al}/^{27}\text{Al}$

ratio of $\sim 5 \times 10^{-5}$) would have been a sufficient heat source for melting planetary bodies a few kilometers in size if accretion happened early enough and ^{26}Al was distributed throughout the solar system (5, 6). It is now known that ^{26}Al is produced in the galaxy at a rather high rate (7), but whether it was broadly available when the solar system formed at the high level corresponding to a $^{26}\text{Al}/^{27}\text{Al}$ ratio of $\sim 5 \times 10^{-5}$ is not clear. The short half-life of ^{26}Al [$t_{1/2} = 0.73$

S. S. Russell and G. J. MacPherson are in the Department of Mineral Sciences, MRC NHB-119, National Museum of Natural History, Smithsonian Institution, Washington, DC 20560, USA. G. Srinivasan, G. R. Huss, and G. J. Wasserburg are in the Lunatic Asylum, Division of Geological and Planetary Sciences, California Institute of Technology, Pasadena, CA 91125, USA.

million years (My)], which decays to ^{26}Mg , makes it possible to use the Al-Mg system as a relative chronometer of early solar system events, provided that Mg isotopic differences between two objects are a function only of formation age or differences in evolutionary history and not of gross nebular isotopic heterogeneities within the solar system. For example, differences in Al-Mg systematics have been used to suggest that the events responsible for forming CAIs and chondrules may have been separated in time by perhaps several million years (8, 9). However, if ^{26}Al was heterogeneously distributed, the observed isotopic differences between chondrules and CAIs could simply be a reflection of that heterogeneity, in which case they would carry no chronologic significance. Clearly, to evaluate the role of ^{26}Al as a heat source and as a relative chronometer of early solar system events, it is necessary to know in detail the abundance and distribution of ^{26}Al in the early solar system.

Understanding the nebular ^{26}Al distribution will require more data from noncarbonaceous chondrites (4). We have systematically searched ordinary chondrites for CAIs and chondrules with phases having high Al/Mg ratios (10) that are suitable for detecting excess ^{26}Mg ($^{26}\text{Mg}^*$) from ^{26}Al decay using secondary ion mass spectrometry (SIMS). Our goals were to compare the isotopic composi-

tions of CAIs and chondrules in ordinary chondrites to each other and to their counterparts in carbonaceous chondrites and to establish, if possible, a relation between formation times of Al-rich chondrules and CAIs. To minimize the possibility of Mg redistribution due to metamorphism, we focused our study on chondrites of petrologic grade 3.6 and lower, that is, those that show little evidence of mineral chemical homogenization.

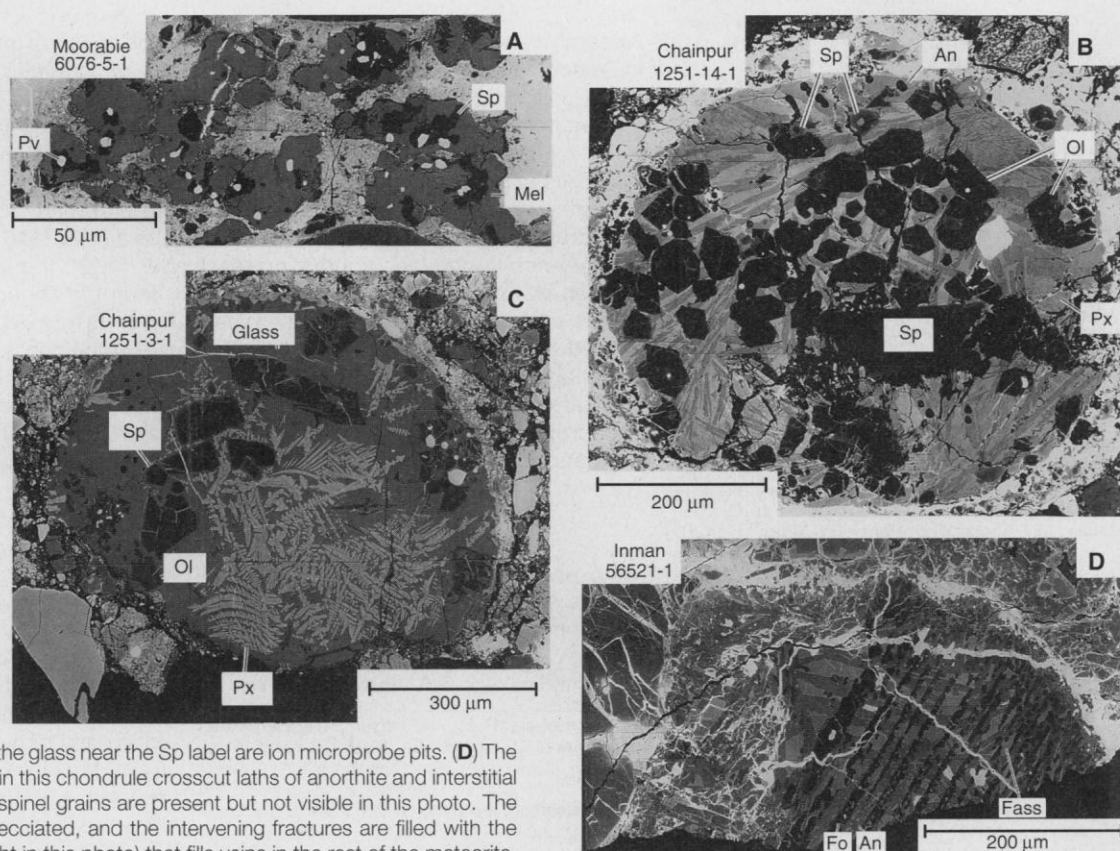
Polished thin sections of H, L, and LL chondrites from the U.S. National Meteorite Collection were examined by optical and electron microscopy. Because CAIs in ordinary chondrites are both rare and small (11), we used systematic x-ray elemental area mapping for Al, Ca, and Mg at a scale sufficient to resolve grains $\sim 5\ \mu\text{m}$ across (12). The chondrules present different problems. Normal ferromagnesian chondrules do not contain primary phases with sufficiently high Al/Mg ratios to permit detection of $^{26}\text{Mg}^*$. We therefore concentrated on searching for chondrules that contain plagioclase as a primary igneous phase; however, we also selected for measurement a chondrule that contains abundant Na-rich glass with a high Al/Mg ratio. Our criteria for recognizing igneous plagioclase were: (i) the feldspar appears texturally to be an early crystallizing phase whose crystalline shapes determine rather than are determined by those of the ferromagnesian phases; (ii) the

plagioclase is calcic in composition, generally bytownite or anorthite rather than the more common sodic varieties produced during chondrite metamorphism; and (iii) the order of appearance of plagioclase in the texturally inferred crystallization sequence accords with that predicted by phase equilibria for a liquid having the bulk composition of the respective host chondrule.

We applied the elemental mapping technique to 22 thin sections from 9 primitive ordinary chondrites, and located 7 Al-rich chondrules and 1 CAI suitable for Al-Mg measurements. We also analyzed a second CAI, identified in the earlier work of Bischoff and Keil (13). We analyzed minerals in these objects with an electron microprobe (14) and calculated bulk compositions of the chondrules using modal mineral abundances (15). Isotopic analyses were performed on suitable minerals (16).

CAIs. The two CAIs we analyzed are from Moorabie (L3.4) and Semarkona (LL3.0). Moorabie 6076-5-1 (Fig. 1A) is a melilite-rich inclusion, petrologically similar to the "Fluffy" Type A inclusions described in CV3 meteorites (17); its bulk composition plots toward the gehlenite end of the field for CV3 CAIs within the $\text{CaO-MgO-Al}_2\text{O}_3\text{-SiO}_2$ (CMAS) tetrahedron (Fig. 2). Semarkona 1805-2-1 is a blue hibonite-rich CAI (11, 13). The mineralogy of this inclu-

Fig. 1. (A) This CAI, imaged with backscattered electrons (as are subsequent photos), consists of clumps of melilite (Mel) that encloses subordinate spinel (Sp), perovskite (Pv), and hibonite (not visible on photo). The individual clumps are separated by intervening meteorite matrix. Each clump has a thin (~ 1 to $2\ \mu\text{m}$) rim of aluminous diopside. (B) Euhedral olivine (Ol) and spinel crystals are dispersed in an ophitic matrix of plagioclase laths (An) enclosed by aluminous diopside pyroxene (Px). Sparse iron-nickel metal beads (bright) are also present. (C) The texture of this chondrule, with its porphyritic spinel and olivine crystals and dendritic aluminous diopside crystals all set in a glassy mesostasis, is spectacular. The small round black spots in the glass near the Sp label are ion microprobe pits. (D) The dark forsteritic olivine bars (Fo) in this chondrule crosscut laths of anorthite and interstitial fassaite (Fass): Rare corroded spinel grains are present but not visible in this photo. The left side of the chondrule is brecciated, and the intervening fractures are filled with the same terrestrial iron oxide (bright in this photo) that fills veins in the rest of the meteorite.



sion resembles those of rare blue hibonite- and melilite-bearing inclusions in Murchison (18); its bulk composition is more SiO_2 -poor and Al_2O_3 -rich than those of CV3 CAIs (Fig. 2). The melilite-spinel pair in Moorabie 6076-5-1 gives a $(^{26}\text{Al}/^{27}\text{Al})_0$ ratio of $(4.9 \pm 1.4) \times 10^{-5}$. The same phases in Semarkona 1805-2-1 give a $(^{26}\text{Al}/^{27}\text{Al})_0$ ratio of $(4.7 \pm 1.5) \times 10^{-5}$. Thus, both CAIs have $^{26}\text{Mg}^*$ abundances (Table 1) consistent with a $(^{26}\text{Al}/^{27}\text{Al})_0$ ratio of $\sim 5 \times 10^{-5}$ (Fig. 3), which is the value observed in most CAIs in carbonaceous chondrites (4). Both CAIs show evidence for mass-dependent fractionation of Mg. The mean Mg isotopic values for spinel and melilite in Moorabie, and for melilite in Semarkona, are ~ 5 per mil per atomic mass unit in favor of the heavy isotopes. The Mg isotopes in spinel in the Semarkona CAI appear to be unfractionated.

Chondrules. All seven of the Al-rich chondrules have textures (19) indicating that they solidified from melt droplets. Two of the chondrules are porphyritic (Chainpur 1251-14-1 and 1251-3-1; Fig. 1, B and C),

one is a barred chondrule (Inman 5652-1-1; Fig. 1D), two have radiating plagioclase textures (Chainpur 1251-14-2 and 5674-2-1), Krymka 1729-9-1 has granular olivine and plagioclase, and Moorabie 6076-5-2 has an intergranular texture. Only for the Moorabie chondrule is there ambiguity about whether it might be a broken fragment of a once-larger object. All but one of the chondrules contain plagioclase that is highly calcic in composition, generally with more than ~ 75 mol% of the anorthite component and in some cases as much as 98% (19). Chainpur 1251-3-1 does not contain plagioclase. Instead, the groundmass consists of Na- and Al-rich glass. The bulk compositions of the Al-rich chondrules differ from those of CAIs and also from those of normal ferromagnesian chondrules. They are more SiO_2 -rich than those of CV3 CAIs (Fig. 2), and many are more MgO-rich as well. In Fig. 2, the Al-rich-chondrule trend does not extend from the CAI trend but, rather, truncates it at a high angle and extends between anorthite and the clustered compositions of Type

1 (MgO-rich) normal chondrules from unequilibrated ordinary chondrites. Therefore, the Al-rich chondrules are intermediate in composition between the Type 1 chondrules and CV3 CAIs, but only in the sense that Al-rich chondrules generally have a higher SiO_2 and MgO content than do the CAIs; the three groups of objects do not define a

Table 1. Al-Mg isotopic data for chondrules and CAI in ordinary chondrites. All errors are 2σ .

Mineral	$\delta^{26}\text{Mg}$ (per mil)	$^{27}\text{Al}/^{24}\text{Mg}$
<i>Semarkona 1805-2-1</i>		
Mel 1	8.9 ± 2.4	21.7 ± 1.5
Mel 2	6.6 ± 1.5	16.5 ± 1.1
Mel 3	5.5 ± 3.8	19.2 ± 1.3
Mel 4	6.5 ± 6.1	29.7 ± 3.3
Mel 5	7.3 ± 2.4	18.5 ± 1.9
Sp 1	2.9 ± 2.8	3.09 ± 0.29
Sp 2	1.3 ± 3.2	3.71 ± 0.35
Sp 3	1.7 ± 2.7	3.79 ± 0.36
Sp 4	2.3 ± 2.6	2.60 ± 0.25
Sp 5	-0.1 ± 2.9	2.95 ± 0.28
<i>Moorabie 6076-5-1</i>		
Mel 2	7.1 ± 4.8	23.9 ± 2.3
Mel 4	5.4 ± 3.5	15.9 ± 1.7
Mel 7	6.2 ± 5.0	31.0 ± 1.8
Mel 8	5.4 ± 5.7	18.5 ± 1.9
Mel 10	20.9 ± 8.2	41.4 ± 4.0
Mel 11	20.8 ± 8.2	58.4 ± 4.17
Sp 1	-0.4 ± 2.7	1.7 ± 0.17
Sp 2	-0.4 ± 2.8	3.2 ± 0.31
Sp 3	0.9 ± 2.3	2.1 ± 0.2
<i>Inman 5652-1-1</i>		
Plag 1	2.2 ± 3.5	42.4 ± 2.0
Plag 2	8.3 ± 6.4	92.7 ± 4.4
Plag 3	1.8 ± 1.8	11.0 ± 0.6
Plag 4	1.2 ± 3.6	29.5 ± 2.2
Plag 5	6.1 ± 5.9	41.3 ± 2.3
Plag 6	2.4 ± 7.0	29.3 ± 2.8
Plag 7	4.7 ± 4.6	33.1 ± 3.5
Plag 8	1.8 ± 4.2	22.2 ± 2.1
Plag 9	2.3 ± 5.3	39.0 ± 3.7
OI	0.7 ± 0.9	$(5.77 \pm 0.04) \times 10^{-3}$
<i>Chainpur 1251-3-1</i>		
OI 1	-0.5 ± 1.5	$(1.48 \pm 0.07) \times 10^{-3}$
OI 2	-0.1 ± 1.4	$(1.62 \pm 0.02) \times 10^{-3}$
OI 3	-0.5 ± 1.4	$(1.65 \pm 0.03) \times 10^{-3}$
Sp 1	-1.5 ± 2.1	2.50 ± 0.08
Sp 2	-0.3 ± 1.9	2.49 ± 0.08
Sp 3	-1.9 ± 1.7	2.60 ± 0.08
Sp 4	-1.1 ± 1.3	2.53 ± 0.08
Sp 5	-0.1 ± 1.7	2.49 ± 0.08
Sp 6	-1.3 ± 2.1	2.54 ± 0.08
Sp 7	-0.2 ± 1.8	2.51 ± 0.08
Gl 1	1.6 ± 4.1	56.7 ± 5.7
Gl 2	3.7 ± 3.7	53.9 ± 5.4
Gl 3	1.6 ± 4.2	52.7 ± 5.3
Gl 4	2.3 ± 3.8	46.5 ± 4.7
Gl 5	3.6 ± 3.5	53.4 ± 5.3
Gl 6	4.1 ± 3.5	53.4 ± 5.4
Gl 7	2.2 ± 3.5	53.0 ± 5.3
Gl 8	3.7 ± 3.8	54.6 ± 5.5
Gl 9	-0.1 ± 3.6	61.7 ± 6.2
Gl 10	2.2 ± 3.1	57.1 ± 5.7
Gl 11	3.3 ± 2.9	64.4 ± 6.5
Gl 12	2.8 ± 2.6	58.5 ± 5.9
Gl 13	1.0 ± 2.5	53.5 ± 5.4

Fig. 2. Bulk compositions of Al-rich chondrules, Type I Mg-rich chondrules [$<2.5\%$ FeO; data from (38)], and CAIs from CV3 chondrites plotted in CMAS (in weight percent). To give better visual reference to the locations of points in the tetrahedron, vertical drop lines are shown for each point; note that these are not projection lines from the Al_2O_3 apex. The thick dashed line is the trajectory for bulk condensed solids from equilibrium condensation calculations (39). Neither Al-rich chondrules nor ferromagnesian chondrules define compositional trends that are particularly consistent with equilibrium condensation.

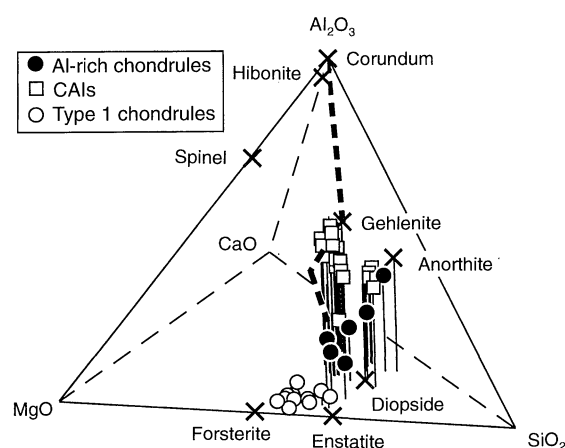
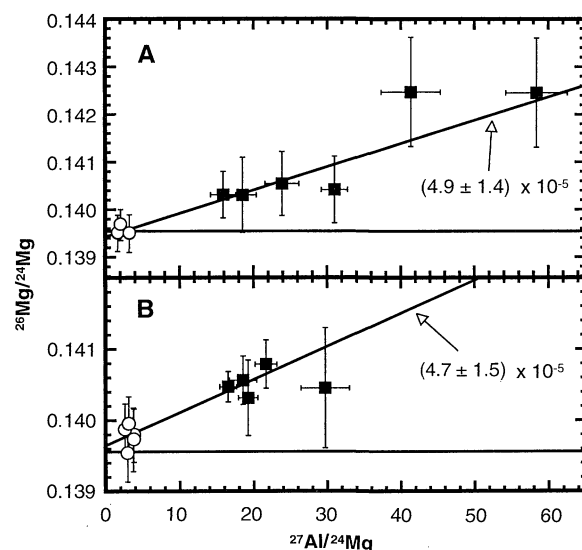


Fig. 3. Al-Mg evolution diagrams for (A) Moorabie 6076-5-1 and (B) Semarkona 1805-2-1. Melilite (filled squares) contains $^{26}\text{Mg}^*$, whereas spinel (open circles) does not. The correlation of $^{26}\text{Mg}/^{24}\text{Mg}$ with $^{27}\text{Al}/^{24}\text{Mg}$ ratios in both of these CAIs indicates that the $^{26}\text{Mg}^*$ was originally incorporated in the CAI as ^{26}Al , which subsequently decayed in situ to ^{26}Mg . The slopes of the correlation lines give the initial ratios $^{26}\text{Al}/^{27}\text{Al}$, which are indistinguishable from 5×10^{-5} .



linear trend. Chainpur 1251-3-1 differs from the other Al-rich chondrules in having $>5\%$ Na_2O by weight and thus does not plot in the CMAS tetrahedron (Fig. 2). It is also enriched in MgO and SiO_2 as compared with the other Al-rich chondrules. All seven of these chondrules therefore differ in mineralogy and bulk composition from normal ferromagnesian chondrules. The genetic relationship between the two types of objects is unclear.

Two Al-rich chondrules contain $^{26}\text{Mg}^*$ (Table 1): Inman 5652-1-1 (Fig. 1D) and Chainpur 1251-3-1 (Fig. 1C). A weighted least-squares regression of the data for Inman 5652-1-1 plagioclase and olivine (Fig. 4A) gives a $(^{26}\text{Al}/^{27}\text{Al})_0$ ratio of $(9.4 \pm 6.3) \times 10^{-6}$. A regression of the olivine, spinel, and glass data for Chainpur 1251-3-1 (Fig. 4B) gives a $(^{26}\text{Al}/^{27}\text{Al})_0$ ratio of $(7.9 \pm 2.7) \times 10^{-6}$. The remaining five chondrules contain no resolvable $^{26}\text{Mg}^*$. Upper limits on $(^{26}\text{Al}/^{27}\text{Al})_0$ ratio for the chondrules are $<4.2 \times 10^{-7}$ for Chainpur 1251-14-2; $<1 \times 10^{-5}$ for Krymka 1729-9; $<2 \times 10^{-6}$ for Chainpur 1251-14-1; $<1.1 \times 10^{-6}$ for Chainpur 5674-2-1; and $<4.1 \times 10^{-6}$ for Moorabie 6076-5-2. No evidence was found in any of these chondrules for mass-dependent isotopic fractionation.

Evidence for ^{26}Al and its significance. Earlier evidence for ^{26}Al in a CAI from an ordinary chondrite came from a hibonite-spinel fragment found in Dhajala (DH-H1)

that yielded a $(^{26}\text{Al}/^{27}\text{Al})_0$ ratio of $(8.4 \pm 0.5) \times 10^{-6}$ (20). Hinton and Bischoff (20) interpreted this result to mean that live ^{26}Al existed in the region where CAIs in ordinary chondrites formed, just as it did in the region where carbonaceous chondrite CAIs formed, but at a substantially reduced level than the latter. Subsequent work on DH-H1 has shown, however, that it is not a typical CAI in terms of its other isotopic properties (4, 21, 22). Our results suggest that most CAIs from ordinary chondrites formed with a $(^{26}\text{Al}/^{27}\text{Al})_0$ ratio of $\sim 5 \times 10^{-5}$, like most CAIs from carbonaceous chondrites. Either Al with that $^{26}\text{Al}/^{27}\text{Al}$ ratio was common to the regions of the nebula where carbonaceous and ordinary chondrite CAIs formed, or else both meteorite groups derived their CAIs from a single source region.

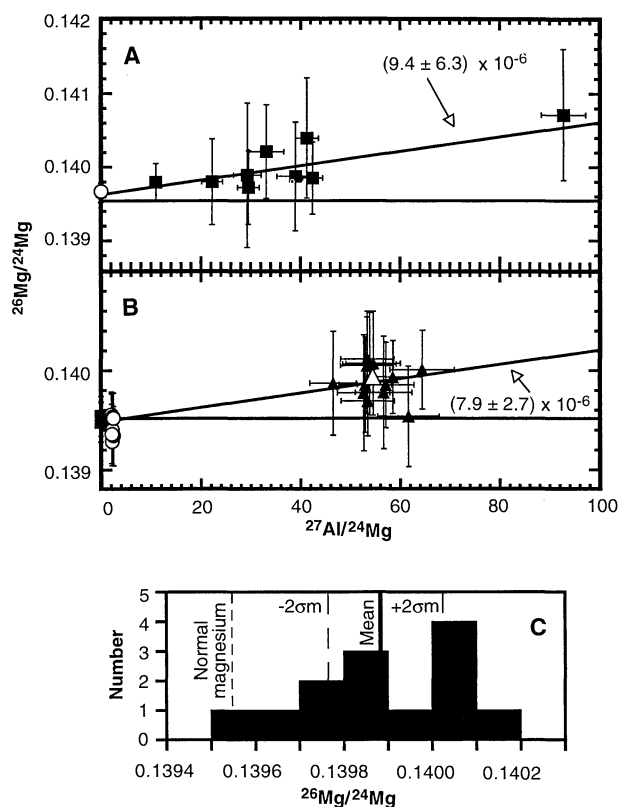
The Al-rich chondrules we analyzed have a much lower $(^{26}\text{Al}/^{27}\text{Al})_0$ ratio than that found in CAIs, and this comparison holds true both across meteorite classes and within individual meteorites such as Allende and Moorabie. Out of 21 Al-rich chondrules and fragments from carbonaceous chondrites (23, 24), only 2 (both from Allende) contained detectable $^{26}\text{Mg}^*$ corresponding to $(^{26}\text{Al}/^{27}\text{Al})_0$ ratios of 6.1×10^{-6} and 2.6×10^{-6} (23). Of several previous measurements of Mg isotopes in non-CAI material from ordinary chondrites (20, 24, 25), only two yielded evidence of the original presence of ^{26}Al : An olivine-pyroxene-anorthite clast

from Semarkona gave a $(^{26}\text{Al}/^{27}\text{Al})_0$ ratio of $(7.7 \pm 2.1) \times 10^{-6}$ (26), and plagioclase crystals (petrologic context unknown) separated from a bulk sample of Saint Marguerite (H4) gave a $(^{26}\text{Al}/^{27}\text{Al})_0$ ratio of $\sim 2 \times 10^{-7}$ (27). Thus, although evidence of ^{26}Al has been found in several chondrules, its original abundance in these chondrules was clearly lower than in CAIs.

The measured difference in $(^{26}\text{Al}/^{27}\text{Al})_0$ ratios between CAIs ($\sim 5 \times 10^{-5}$) and $^{26}\text{Mg}^*$ -bearing chondrules ($\sim 1 \times 10^{-5}$) has been variously interpreted in terms of (i) differing degrees of isotopic resetting, by later metamorphism, in groups of objects that formed contemporaneously (28); (ii) contemporaneous formation from reservoirs with different $(^{26}\text{Al}/^{27}\text{Al})_0$ ratios [for example, (29)]; and (iii) differences in times of formation from an isotopically homogeneous reservoir (4, 8, 24, 30). We consider each of these interpretations in turn.

If the isotopic difference between CAIs and chondrules is a result of later preferential resetting of the Al-Mg isotopic systems in the chondrules by element redistribution, then the inferred $(^{26}\text{Al}/^{27}\text{Al})_0$ ratios give no information about the formation interval between CAIs and chondrules but instead refer to the time of elemental redistribution during metamorphism. Wood (28) has advocated this interpretation primarily because of the astrophysical difficulties of storing CAIs in the nebula for 2 My before chondrules begin to form, without their falling into the sun as a result of drag-induced radial drift. Because of the need to minimize the influence of metamorphism, our study, and that of Hutcheon and Jones (24), concentrated on chondrules of low metamorphic grade and looked for chondrules with igneous plagioclase or undivertified Al-rich glass. The finding of $^{26}\text{Mg}^*$ in the feldspathic glass of the Chainpur chondrule 1251-3-1, but not in three other chondrules from the same meteorite, suggests that indeed metamorphism was not responsible for the observed isotopic patterns. The glass should have been more susceptible to diffusive redistribution of Mg during metamorphism than the plagioclase. Chainpur (LL3.4) probably never experienced temperatures significantly in excess of $\sim 400^\circ\text{C}$ (31), and calculations of diffusion rates for Mg in plagioclase suggest that Mg isotopes should not have been disturbed at that peak temperature. At 400°C , Mg isotopes in a plagioclase grain large enough to measure by SIMS ($\sim 50 \mu\text{m}$) cannot be equilibrated over the age of the solar system [for a diffusivity $D = 1 \times 10^{-27} \text{ cm}^2/\text{s}$, by analogy to strontium in anorthite; (32)]. Therefore, the Mg isotopes of the chondrules must reflect the values at the time of incorporation into the parent body. It is possible that some of the Chainpur chondrules had their Al-Mg clocks reset prior to

Fig. 4. Al-Mg evolution diagrams for the Al-rich chondrules. (A) Inman 5652-1-1 contains $^{26}\text{Mg}^*$ -bearing plagioclase (filled squares) and olivine (open circle) that has a terrestrial $^{26}\text{Mg}/^{24}\text{Mg}$ ratio. (B) Chainpur 1251-3-1 contains $^{26}\text{Mg}^*$ -bearing glass (filled triangles), and olivine (filled squares) and spinel (open circles) that have a terrestrial $^{26}\text{Mg}/^{24}\text{Mg}$ ratio. Although the cluster of glass analyses from Chainpur 1251-3-1 shows considerable overlap with a zero-slope line, the weighted mean (open triangle) is well resolved from zero. The indicated slopes for (A) and (B), corresponding to initial $^{26}\text{Al}/^{27}\text{Al}$ ratios, are based on weighted regressions. (C) $^{26}\text{Mg}/^{24}\text{Mg}$ measurements for glass from Chainpur 1251-3-1. The weighted mean of the analyses is resolved from normal Mg by $> 2\sigma$.



accretion, either in the nebula or in earlier formed bodies. However, if CAIs and chondrules formed from the same isotopic reservoir, then the Chainpur chondrule with $^{26}\text{Mg}^*$ must have formed, or had its Al-Mg system reset, ~ 2 My after the formation of CAIs, and the Chainpur parent body must have been assembled >5 My after the formation of CAIs.

An alternative possibility is that the isotopic difference between CAIs and chondrules arose from isotopic heterogeneities in the nebula. The most familiar variant of such a model is that ^{26}Al was irregularly distributed because of incomplete mixing of presolar components. For example, Wood (28) pointed out that the Al-Mg data for chondrules comes primarily from ordinary chondrites whereas that for CAIs comes from carbonaceous chondrites. This difference implies that the accretion regions of the two chondrite groups might have been isotopically different. However, our data demonstrate that CAIs from unequilibrated ordinary chondrites and carbonaceous chondrites commonly had the same $(^{26}\text{Al}/^{27}\text{Al})_0$ ratio. Moreover, Sheng *et al.*'s (23) demonstration that Al-rich chondrules from Allende had low or zero $(^{26}\text{Al}/^{27}\text{Al})_0$ ratios means that CAIs and chondrules from a single accretion region must have differed in their original ^{26}Al abundance. We therefore think that it is unlikely that the Mg isotopic differences between CAIs and chondrules can be attributed to isotopic differences in the respective accretion regions of ordinary and carbonaceous chondrites.

A different variant of the nebular heterogeneity model is that chondrules and CAIs formed from chemically and isotopically different fractions of a well-mixed dust reservoir in which the ^{26}Al was largely sited in refractory dust. Evaporation of dust mixtures would preferentially drive off the volatile constituents, enriching the residue in refractory elements and ^{26}Al . Chondrules would form from less chemically fractionated material, and CAIs from the more fractionated, less volatile residue. A problem with this model is the ubiquitous value for the $(^{26}\text{Al}/^{27}\text{Al})_0$ ratio of $\sim 5 \times 10^{-5}$ that is observed in CAIs covering a wide range of bulk composition: The model not only predicts a wide range of $(^{26}\text{Al}/^{27}\text{Al})_0$ ratios but also a correlation between $(^{26}\text{Al}/^{27}\text{Al})_0$ and bulk composition.

Yet a third variant of nebular heterogeneity is that there was local production of ^{26}Al in the nebula. Clayton and Jin (29) suggested that ^{26}Al in the early solar system was produced by energetic particles from the sun irradiating a thin layer of the nebula. Only refractory CAIs would form in this high-temperature, low-density environment, and in particular, would necessarily do so late in order to accumulate sufficient ^{26}Al . In this model, the relative ^{26}Al con-

centrations in chondrules and CAIs would reflect distances from the irradiated shell and not time differences; indeed, CAIs could actually form later than the chondrules. Because the model requires that the irradiation affects small grains that are then assembled into larger objects, it suffers from the difficulty of making centimeter-sized CAIs with a range of chemical compositions that have the same $(^{26}\text{Al}/^{27}\text{Al})_0$ ratio ($\sim 5 \times 10^{-5}$). One implication of the model is that CAIs with non-radiogenic nuclear anomalies in other elements but no $^{26}\text{Mg}^*$ must form in a different place by a completely different process than normal CAIs.

Interpreting the differences in $(^{26}\text{Al}/^{27}\text{Al})_0$ ratios among objects or groups of objects in chronologic terms requires that: (i) all objects formed from a single, isotopically homogeneous, reservoir; (ii) each individual object was a cogenetic mineral assemblage; and (iii) the objects subsequently remained closed systems over solar system history with respect to Mg or Al exchange, either between the constituent mineral phases or with the outside environment. Our observations show that chondrules and CAIs satisfy the first requirement to the extent that ordinary and carbonaceous chondrite CAIs formed with similar $(^{26}\text{Al}/^{27}\text{Al})_0$ ratios to each other, and chondrules likewise, indicating that different accretion regions did not differ substantially with respect to Al isotopes. However, our data do not by themselves preclude a model in which chondrules and CAIs formed in separate and isotopically different regions, then remixed equally into all of the various accretion regions [for example, (29)]. Because chondrules and many CAIs solidified from molten droplets, an assumption of initial homogeneity in each individual object is probably reasonable [the case for CAIs has been discussed in detail elsewhere (1, 4)]. With respect to isotopic resetting or exchange, many CAIs certainly have experienced secondary events that caused varying degrees of isotopic resetting of the Al-Mg system. However, in most cases a signature of the original isotopic composition is preserved, which is why the $(^{26}\text{Al}/^{27}\text{Al})_0$ ratio of $\sim 5 \times 10^{-5}$ is observed through the CAI population (4). The chondrules may well have experienced some resetting as well, but the variability in isotopic compositions within just a single relatively unmetamorphosed chondrite (Chainpur) suggests that any resetting was preaccretionary. Moreover, within the subset of chondrules that contain resolved $^{26}\text{Mg}^*$, a rather consistent isotopic signature in which the $(^{26}\text{Al}/^{27}\text{Al})_0$ ratio is $\sim 1 \times 10^{-5}$ is beginning to be recognized [(23); this study]. Interpreted in terms of formation time with the above stated assumptions, the measured

levels of $^{26}\text{Mg}^*$ corresponding to $(^{26}\text{Al}/^{27}\text{Al})_0 \sim 1 \times 10^{-5}$ in the Chainpur and Inman chondrules constrain formation of those objects to have taken place ~ 2 My after the formation of CAI with a $(^{26}\text{Al}/^{27}\text{Al})_0$ ratio of $\sim 5 \times 10^{-5}$.

Constraints of the solar nebula time scale, and on chondrule and CAI formation. The demonstration that the Al-rich chondrules and CAIs from ordinary chondrites are like their counterparts in carbonaceous chondrites in terms of their Mg-isotope systematics implies that the nebula was not spatially heterogeneous in its $^{26}\text{Al}/^{27}\text{Al}$ ratio on any large scale as a result of grossly incomplete mixing of presolar components. We can now argue that the ordinary and carbonaceous chondrite accretion regions were similar in $^{26}\text{Al}/^{27}\text{Al}$ ratios in the respective CAI and chondrule components. It remains to be established how representative these materials are of the asteroid belt or, for that matter, of the solar system. The isotopic differences between chondrules and CAIs are most plausibly a result of differences in formation time, rather than selective reprocessing and resetting of chondrule isotope systems relative to those in CAIs. Our results do not by themselves rule out heterogeneity models in which chondrules and CAIs formed either from different volatility controlled fractions of nebular dust or in distinct and isotopically different locales. If the isotopic differences between the two groups of objects reflect age differences, then Al-rich chondrules were forming 2 My after formation of most CAIs. If CAIs and Al-rich chondrules are both nebular products, then this time span is a minimum duration for the nebular phase of the solar system. Isotopic differences among the four Chainpur chondrules indicate that the Chainpur parent body must have been assembled >5 My after the formation of CAIs. Any resetting of the isotope systems in those Chainpur chondrules with no detectable $^{26}\text{Mg}^*$ did not occur in the Chainpur parent body; it either happened in the nebula or else took place in an earlier generation of the parent body, prior to accretion of Chainpur.

We have related the $^{26}\text{Al}/^{27}\text{Al}$ ratios to the nebular time scales; however, the mechanisms that produce chondrules and CAIs and their connection with the nebular dust are not resolved. There are no self-consistent models for explaining the chemical composition of the diverse chondrule types. Shu *et al.* (33) proposed that different chondrules and CAIs were formed during the disc inflow by aerodynamic drag on small bodies, which lifts them from the shaded disc to expose them to radiation during the bipolar outflow. Depending on the trajectories, particles are heated to varying degrees and some are launched and return back to the disk.

This avoids the problem of heating the disk to high temperatures at large radial distances from the sun. For this appealing model, there is a direct connection between chondrule and CAI production and the lifetime of the accretion disc. The inferred nebular time scales from ^{26}Al and the dynamical model are in reasonable accord. However, this depends on the ^{26}Al responsible for the observed $^{26}\text{Mg}^*$ being initially present. If it were produced (along with other nuclei) during ejection on a rather short time of exposure to varying degrees of proton bombardment, then the time scale inferred from the $^{26}\text{Al}/^{27}\text{Al}$ ratio would not apply.

REFERENCES AND NOTES

1. T. Lee, D. A. Papanastassiou, G. J. Wasserburg, *Geophys. Res. Lett.* **3**, 109 (1976).
2. ———, *Astrophys. J.* **228**, L93 (1979).
3. G. J. Wasserburg, T. Lee, D. A. Papanastassiou, *Geophys. Res. Lett.* **4**, 299 (1977).
4. G. J. MacPherson, A. M. Davis, E. K. Zinner, *Meteoritics* **30**, 365 (1995).
5. H. C. Urey, *Proc. Natl. Acad. Sci. U.S.A.* **41**, 127 (1955).
6. M. T. Bernius, I. D. Hutcheon, G. J. Wasserburg, *Lunar Planet. Sci.* **XXII**, 93 (1991).
7. W. A. Mahoney, J. C. Ling, W. A. Wheaton, A. S. Jacobsen, *Astrophys. J.* **286**, 578 (1984); R. Diehl et al., *Astrophys. J. Suppl.* **92**, 429 (1994).
8. A. G. W. Cameron, *Meteoritics* **30**, 133 (1995).
9. I. D. Hutcheon, G. R. Huss, G. J. Wasserburg, *Lunar Planet. Sci.* **XXV**, 587 (1994).
10. G. Srinivasan, S. S. Russell, G. J. MacPherson, G. R. Huss, G. J. Wasserburg, *Lunar Planet. Sci.* **XXVII**, 1257 (1996).
11. G. J. MacPherson, D. A. Wark, J. T. Armstrong, in *Meteorites and the Early Solar System*, J. F. Kerridge and M. S. Matthews, Eds. (Univ. of Arizona Press Tucson, AZ, 1988).
12. Samples were examined with a JEOL 840a scanning electron microscope at the Smithsonian Institution. Location maps were constructed from backscattered electron (BSE) photomosaics of entire thin sections. X-ray maps were made using a Fisons/KeveX Sigma energy-dispersive x-ray analysis system attached to the SEM.
13. A. Bischoff and K. Keil, *Geochim. Cosmochim. Acta* **48**, 693 (1984).
14. Mineral chemistry was analyzed using an ARL-SEMQ automated 9-spectrometer electron microprobe at the Smithsonian, operated at 15 kV accelerating potential and 0.15 μA beam current. Counting times were 40 seconds. Natural and synthetic crystalline materials were used as calibration standards. Data were corrected for matrix, absorption, and atomic number effects using a phi-rho-z program.
15. The bulk composition of each chondrule was calculated by combining a point-count mode with analyzed mineral compositions and appropriate mineral densities. Area fraction is assumed to be equivalent to volume fraction.
16. Isotopic analyses were made with the Caltech "P-nurture" Cameca ims3f ion microprobe (34). Because of the small grain size of the Al-rich phases in the chondrules and CAIs, enhanced spatial resolution was essential to achieving uncontaminated analyses of individual phases. Primary beam spot diameters of ~ 2 to $3 \mu\text{m}$ were achieved by employing low beam currents (0.1 to 0.5 nanoamps) and carefully tuning the primary ion column. In some cases an $8\text{-}\mu\text{m}$ field aperture was used to minimize ion contributions from adjacent high-Mg phases. ^{26}Mg excesses are reported as $\delta^{26}\text{Mg}$, the deviations in parts-per-thousand (per mil: ‰) from terrestrial Mg

$$\delta^{26}\text{Mg} = [(^{26}\text{Mg}/^{24}\text{Mg})_c / 0.13955] - 1 \times 1000$$
 where $(^{26}\text{Mg}/^{24}\text{Mg})_c$ is the measured ratio corrected for fractionation by normalizing to $^{26}\text{Mg}/^{24}\text{Mg} = 0.12663$ (35) using a "linear law" (4), and 0.13955 is taken as the fractionation-corrected $^{26}\text{Mg}/^{24}\text{Mg}$ of terrestrial standards as measured on the Caltech ion probe (36).
17. G. J. MacPherson and L. Grossman, *Geochim. Cosmochim. Acta* **48**, 29 (1984).
18. G. J. MacPherson, M. Bar-Matthews, T. Tanaka, E. Olsen, L. Grossman, *ibid.* **47**, 823 (1983).
19. Semarkona 1805-2-1 is a lens-shaped and compact CAI $\sim 480 \mu\text{m}$ in maximum dimension, that consists of densely intergrown blue-pleochroic hibonite laths ($\text{TiO}_2 \sim 3$ to 7% ; MgO up to 3%) ~ 20 to $40 \mu\text{m}$ across, and smaller irregular melilite (Al_{1-10}) perovskite, and spinel (FeO up to 0.4%). The inclusion has a mantle of melilite (Al_{1-18}) and a discontinuous layered rim sequence of anorthite (An_{98}) and fassaite. One portion of the inclusion is fragmented and porous. Chainpur 5674-2-1 is a circular chondrule $500 \mu\text{m}$ across dominated by large plagioclase laths (An_{78-97}) up to $350 \mu\text{m}$ long and $65 \mu\text{m}$ wide. The cores of the laths have been mostly replaced by nepheline. Interstitial to the plagioclase are sparse blocky olivine grains (interior: Fo_{99-98}), some with hollow cores, and blocky to branching aluminous diopside ($\text{Al}_2\text{O}_3 \sim 10\%$, $\text{TiO}_2 \sim 3\%$); in the centers of the interstices are dendritic intergrowths of olivine and plagioclase in some places and diopside and plagioclase in others. There is a small amount of residual glass. Near the exterior of the chondrule, the olivine crystals are iron-rich (Fo_{90}) along grain margins and fractures, probably the result of mild metamorphism. The texturally inferred order of appearance of crystallizing phases is plagioclase, followed by olivine and pyroxene. The crystallization sequence inferred from phase equilibria is similar but includes spinel as the second phase to appear. However, spinel is in a reaction relationship with the melt once forsterite appears (37) and may have reacted away prior to final solidification. Chainpur 1251-14-2 is an irregularly shaped chondrule $\sim 300 \mu\text{m}$ in maximum dimension. It is composed mainly of large plagioclase laths up to $\sim 185 \mu\text{m}$ long (An_{90-97}), partially to largely altered to nepheline, and riddled with submicron-sized round holes. Interstitial to the feldspar laths is a coarse intergrowth of plagioclase and aluminous diopside ($\text{Al}_2\text{O}_3 \sim 26\%$, $\text{TiO}_2 = 3\text{--}4\%$). Chainpur 1251-14-1 is a somewhat elliptical chondrule $600 \mu\text{m}$ across (Fig. 1B). It is composed of abundant large (up to $85 \mu\text{m}$) euhedral olivine crystals (Fo_{96-99} in interior) and sparse spinel grains that are locally embayed and corroded ($\text{FeO} = 1\%$; most $< 30 \mu\text{m}$, but one central crystal is $185 \mu\text{m}$). Occurring interstitially to olivine and spinel are subhedral to euhedral plagioclase laths (An_{82-90}) optically enclosed in aluminous diopside ($\text{Al}_2\text{O}_3 \sim 13\%$, $\text{TiO}_2 \approx 3\%$). Sparse iron-nickel metal beads are also present. Some spinel grains are enclosed by forsterite. Plagioclase laths are without exception truncated where they abut forsterite and spinel. The texturally inferred crystallization sequence is spinel, olivine, plagioclase, and then pyroxene, in general agreement with that predicted by phase equilibria for a melt of this composition, provided that not all of the spinel reacts with the melt upon the appearance of anorthite as a crystallizing phase. Chainpur 1251-3-1 is a round chondrule $850 \mu\text{m}$ in maximum dimension that is broken on one side (Fig. 1C). It has a porphyritic texture, with equant spinel (up to $\sim 125 \mu\text{m}$) and equant to skeletal olivine (up to $\sim 290 \mu\text{m}$) crystals set in a mesostasis of glass and dendritic aluminous diopside crystals. Moorabie 5-2 is a rounded $575\text{-}\mu\text{m}$ chondrule composed of blocky olivine crystals up to $\sim 130 \mu\text{m}$ in size (Fo_{80-83}) that are partially to completely mantled by Mg-rich subcalcic augite ($\text{Wo}_{17}\text{En}_{66}\text{Fs}_{17}$). Interstitial to these are anhedra, partly maskelynitized plagioclase laths up to $\sim 100 \mu\text{m}$ in length. The texturally inferred crystallization sequence was olivine, then pigeonite, and finally anorthite. The crystallization sequence predicted by phase equilibria is in general agreement except that low Ca pyroxene (enstatite) is the expected pyroxene phase rather than subcalcic augite. Krymka 9-1 is a rounded chondrule, just over 1 mm in diameter, composed mostly of blocky olivine grains (Fo_{82-87}) with interstitial anhedra plagioclase (An_{83-95}). In the interior of the chondrule are rare grains of a pyroxene, presumably pigeonite, that has exsolved to enstatite and augite. Minor enstatite grains ($\text{FeO} = 9\%$) occur around the periphery of the chondrule, rimming olivine. The texturally inferred crystallization sequence is olivine, plagioclase or enstatite, and finally pigeonite, in general agreement with phase equilibria predictions. Moorabie 6076-5-1 is a $\sim 170\text{-}\mu\text{m}$ (maximum dimension) discontinuous CAI (Fig. 1A) that consists of several discrete clumps of melilite (Al_{1-5}) that encloses subordinate spinel (FeO up to 2%), blocky $\sim 2\text{--}4\text{-}\mu\text{m}$ -sized perovskite grains, and rare $\sim 10\text{-}\mu\text{m}$ -long hibonite. The individual clumps are separated by intervening meteorite matrix. Each clump has a thin (~ 1 to $2 \mu\text{m}$) rim consisting of aluminous diopside. Inman 5652-1-1 is a rounded chondrule $\sim 500 \mu\text{m}$ in diameter that has a barred olivine structure (Fig. 1D). The skeletal olivine bars (Fo_{78-98}) cut across laths of anorthite (An_{96-98}) that locally are subparallel to one another and nearly perpendicular to the olivine, giving parts of the chondrule a cross-barred texture. Interstitial to the feldspar is aluminous diopside ($\text{Al}_2\text{O}_3 = 15\text{--}22\%$; $\text{TiO}_2 = 1$ to 1.6%). Rare, corroded spinel grains are enclosed in plagioclase and pyroxene. The texturally inferred order of appearance of crystallizing phases is olivine or spinel first, followed by plagioclase (spinel out by reaction), and finally pyroxene. The melt composition is, however, significantly undersaturated with respect to olivine at the liquidus, suggesting that substantial undercooling controlled the order of crystallization and textures in this object.
20. R. W. Hinton and A. Bischoff, *Nature* **308**, 169 (1984).
21. R. N. Clayton, R. W. Hinton, A. M. Davis, *Philos. Trans. R. Soc. London Ser. A* **325**, 483 (1988).
22. R. W. Hinton, A. M. Davis, D. E. Scatena-Wachel, L. Grossman, R. J. Druas, *Geochim. Cosmochim. Acta* **52**, 2573 (1988).
23. Y. J. Sheng, I. D. Hutcheon, G. J. Wasserburg, *ibid.* **55**, 581 (1991).
24. I. D. Hutcheon and R. H. Jones, *Lunar Planet. Sci.* **XXVI**, 647 (1995).
25. I. D. Hutcheon, R. Hutchison, A. Kennedy, *ibid.* **XX**, 434 (1989).
26. I. D. Hutcheon and R. Hutchison, *Nature* **337**, 238 (1989).
27. E. K. Zinner and C. Göpel, *Meteoritics* **27**, 311 (1992).
28. J. A. Wood, in *Chondrules and the Protoplanetary Nebula*, R. Hewins, Ed. (Cambridge Univ. Press, Cambridge, 1996), p. 55.
29. D. D. Clayton and L. Jin, *Astrophys. J.* **451**, L87 (1995).
30. T. D. Swindle, A. M. Davis, C. M. Hohenberg, G. J. MacPherson, L. E. Nyquist, in (28), p. 77.
31. D. W. G. Sears, F. A. Hasan, J. D. Batchelor, J. Lu, *Proc. Lunar Planet. Sci. Conf.* **21**, 493 (1991).
32. D. J. Cherniak and E. B. Watson, *Earth Planet. Sci. Lett.* **113**, 411 (1992).
33. F. H. Shu, H. Shang, T. Lee, *Science* **271**, 1545 (1996).
34. A. J. Fahey, E. K. Zinner, G. Crozaz, A. Kornacki, *Geochim. Cosmochim. Acta* **51**, 3215 (1987).
35. E. J. Catanzaro, T. J. Murphy, E. L. Garner, W. R. Shields, *J. Res. Natl. Bur. Standards* **70A**, 453 (1966).
36. C. A. Brigham, thesis, California Institute of Technology (1990).
37. Y. J. Sheng, thesis, California Institute of Technology (1991).
38. R. H. Jones and E. R. D. Scott, *Proc. Lunar Planet. Sci. Conf.* **19**, 523 (1989).
39. L. Grossman, *Geochim. Cosmochim. Acta* **36**, 597 (1972).
40. We thank A. M. Davis and an anonymous reviewer for comments that significantly improved this paper. This research was supported by NASA grants NAGW 3553 (G.J.M.) and NAGW 3297 (G.J.W.). This is Caltech contribution no. 5679 (934).

23 April 1996; accepted 17 July 1996